Expanded View Figures

Figure EV1. Transcriptome analysis of yeast OXPHOS mutants. Related to Fig 1.

A Gene ontology analysis of significantly changed transcripts in ρ^0 cells (*P* value < 0.05).

B Gene ontology analysis of significantly changed transcripts encoding mitochondrial proteins in ρ^0 cells (*P* value < 0.05).

C Heat map plots of the mRNA level changes of genes encoding selected functional groups of mitochondrial proteins (gene list in Table EV1C) in the OXPHOS mutants. Gray boxes: deleted genes (*COR1*, *COX9*, and *ATP7*).

© 2021 The Authors

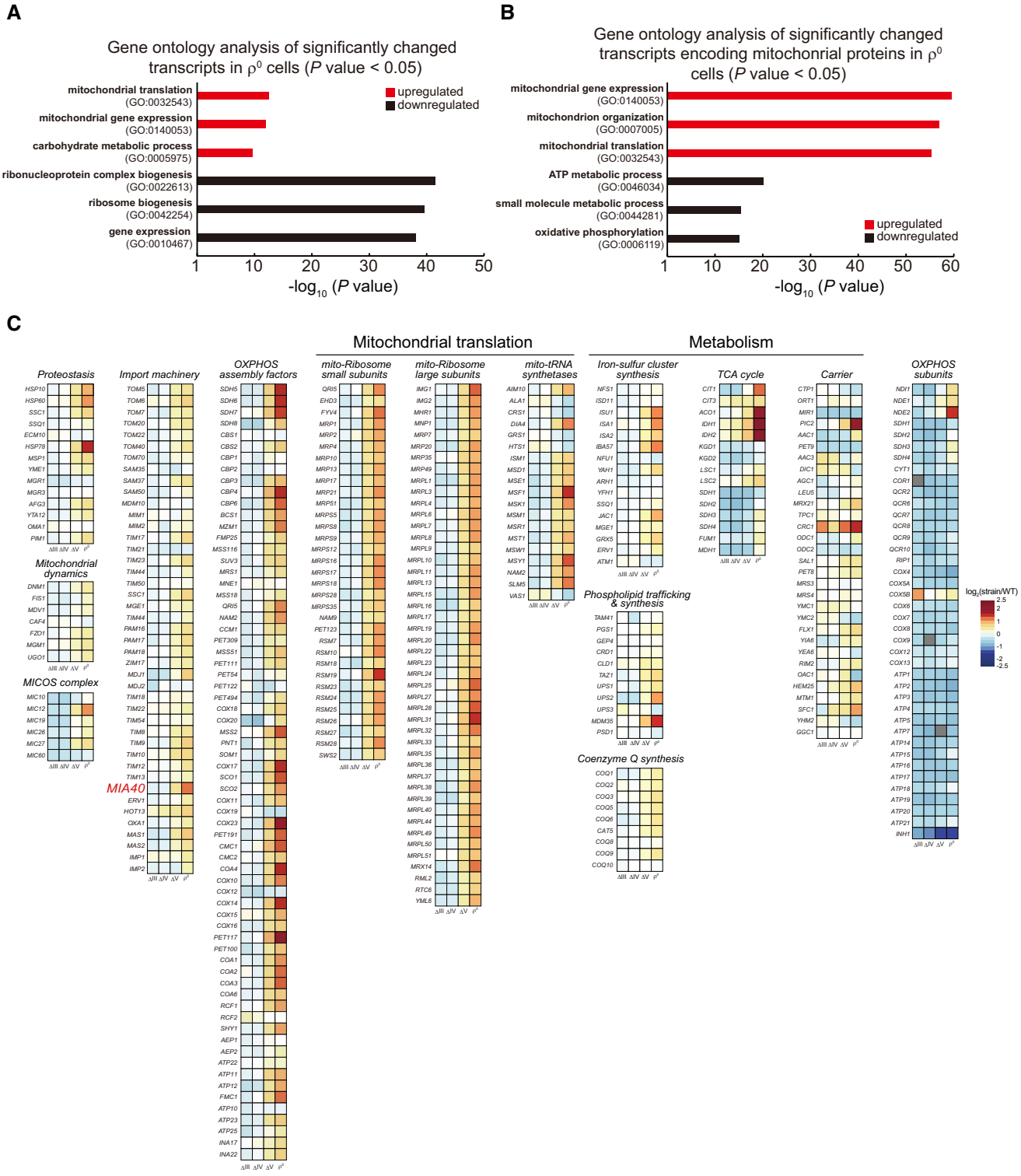
A
Gene ontology analysis of significantly changed transcripts in ρ0 cells (P value < 0.05)
mitochondrial translation (GO:0032543)
mitochondrial gene expression (GO:0140053)
carbohydrate metabolic process (GO:0005975)
ribonucleoprotein complex biogenesis (GO:0022613)
ribosome biogenesis (GO:0042254)
gene expression (GO:0010467)
upregulated
downregulated
1 10 20 30 40 50
-log10 (P value)
B
Gene ontology analysis of significantly changed transcripts encoding mitochonrial proteins in ρ0 cells (P value < 0.05)
mitochondrial gene expression (GO:0140053)
mitochondrion organization (GO:0007005)
mitochondrial translation (GO:0032543)
ATP metabolic process (GO:0046034)
small molecule metabolic process (GO:0044281)
oxidative phosphorylation (GO:0006119)
upregulated
downregulated
1 10 20 30 40 50 60
-log10 (P value)
C
Mitochondrial translation
Metabolism
Proteostasis
Import machinery
OXPHOS assembly factors
mito-Ribosome small subunits
mito-Ribosome large subunits
mito-tRNA synthetases
Iron-sulfur cluster synthesis
TCA cycle
Carrier
OXPHOS subunits
Mitochondrial dynamics
MICOS complex
Phospholipid trafficking & synthesis
Coenzyme Q synthesis
MIA40
log2(strain/WT)

Figure EV1.

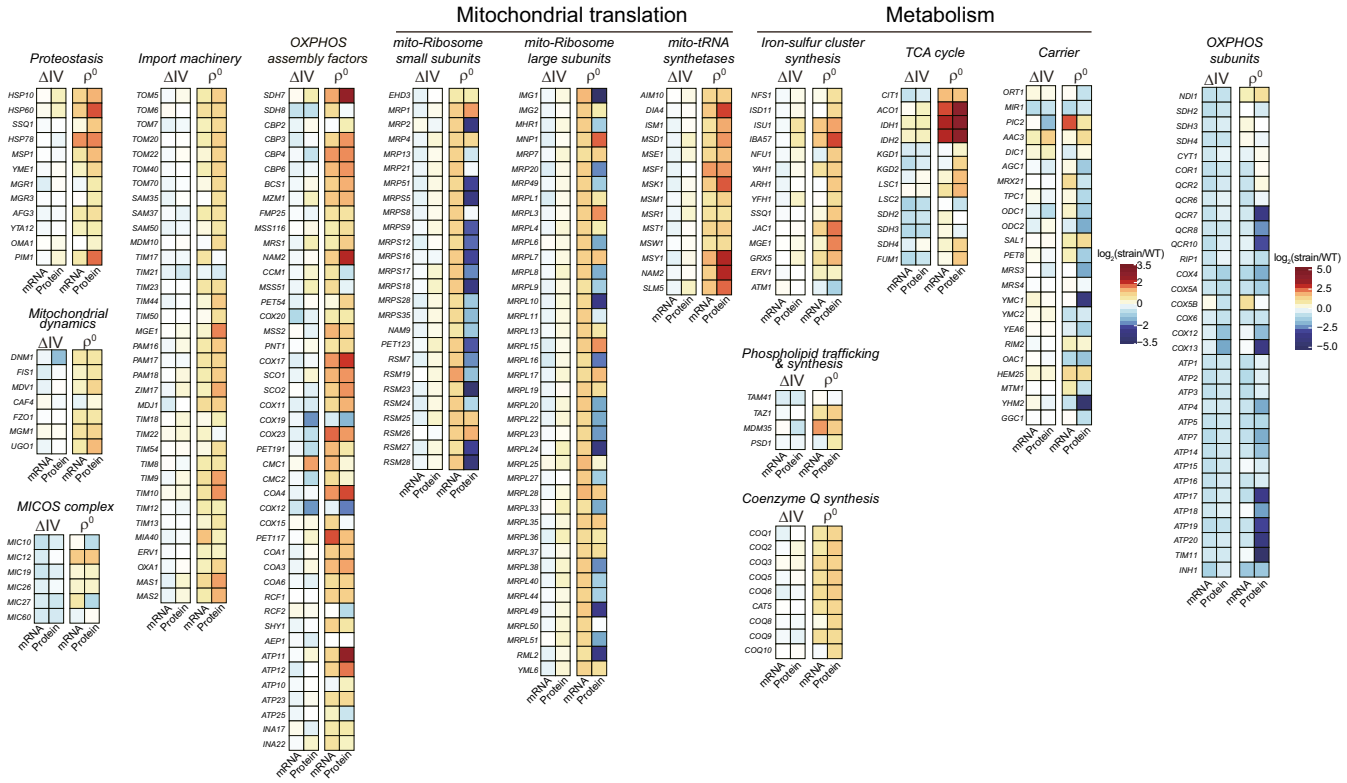

Figure EV2. Correlation between mRNA and protein level changes of selected mitochondrial proteins. Related to Fig 2.

Heat map plots of the mRNA and protein level changes of genes encoding selected functional groups of mitochondrial proteins (gene list in Table EV1C) in the ΔIV and ρ^0 cells.

© 2021 The Authors

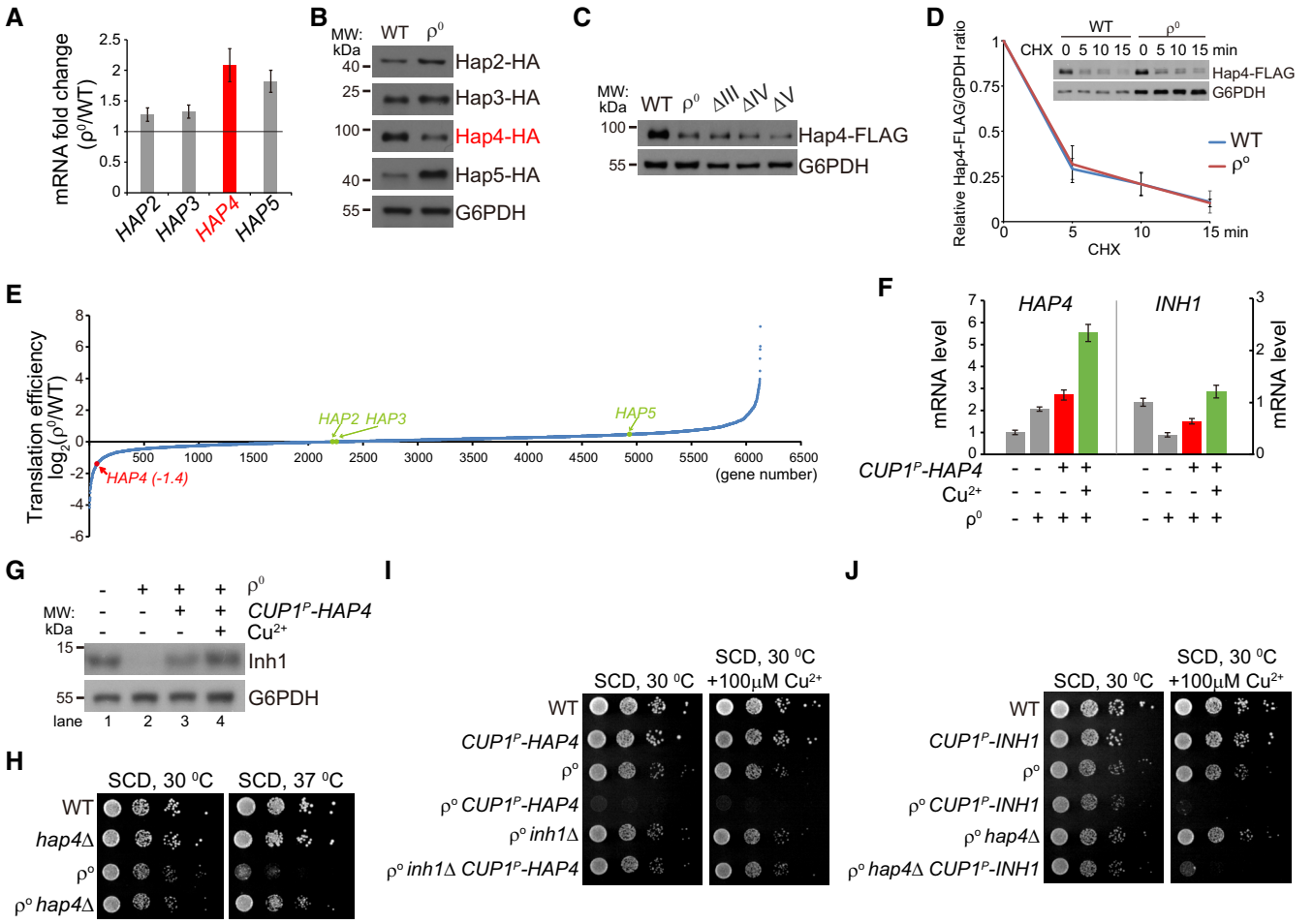

Figure EV3. Translational downregulation of Hap4 represses transcription of *INH1*. Related to Fig 3.

A qRT–PCR analysis of HAP complex components in ρ^0 cells. Data are mean ± SD from three biological replicates. The horizontal line indicates fold change of 1.

B Western blot analysis of Hap proteins. Hap proteins were endogenously tagged with HA. Whole cell lysates were extracted, and equal amount of proteins was loaded for Western blot.

C Western blot analysis of Hap4-FLAG level in OXPHOS mutants. Hap4 was endogenously tagged with FLAG. Whole cell lysates were extracted, and equal amount of proteins was loaded for Western blot.

D Protein half-life of Hap4-FLAG is not changed in ρ^0 cells as compared to WT cells. Hap4 was endogenously tagged with FLAG. Cells were treated with cycloheximide (CHX) to block protein synthesis for the indicated time. Whole cell lysates were extracted for Western blot analysis. Protein samples of ρ^0 cells were loaded twofold the amounts of samples of WT cells to equalize Hap4-FLAG amount at 0 min of CHX treatment. Relative Hap4-FLAG/G6PDH ratio at 0 min of CHX treatment was normalized as 1. Data are mean ± SD from three biological replicates.

E Genome-wide translation efficiency changes in ρ^0 cells versus WT cells (Dataset EV3). The translation efficiencies of Hap proteins are indicated.

F qRT–PCR analysis of *HAP4* and *INH1* mRNA levels upon Hap4 overexpression in the indicated strains. A cassette expressing Hap4 under the control of *CUP1* promoter was inserted into the HO locus. Hap4 overexpression was induced by 100 μM $CuSO_4$ for 12 h. Data are mean ± SD from three biological replicates.

G Western blot analysis of Inh1 level upon Hap4 overexpression in the indicated strains. Whole cell lysates were extracted, and equal amount of proteins was loaded for Western blot.

H Deletion of *HAP4* benefits the proliferation of ρ^0 cells at 37°C. Serial dilutions (tenfold dilution) of the indicated strains were analyzed on SCD plates at 30°C and 37°C for 2 days.

I Overexpression of Hap4 inhibits the proliferation of ρ^0 cells, but not the proliferation of ρ^0 *inh1*Δ cells.

J Overexpression of Inh1 inhibits the proliferation of both ρ^0 and ρ^0 *hap4*Δ cells.

Data information: Serial dilutions (tenfold dilution) of the indicated strains were analyzed on SCD or SCD plus 100 μM $CuSO_4$ plates at 30°C for 2 days (I, J).

Source data are available online for this figure.

© 2021 The Authors

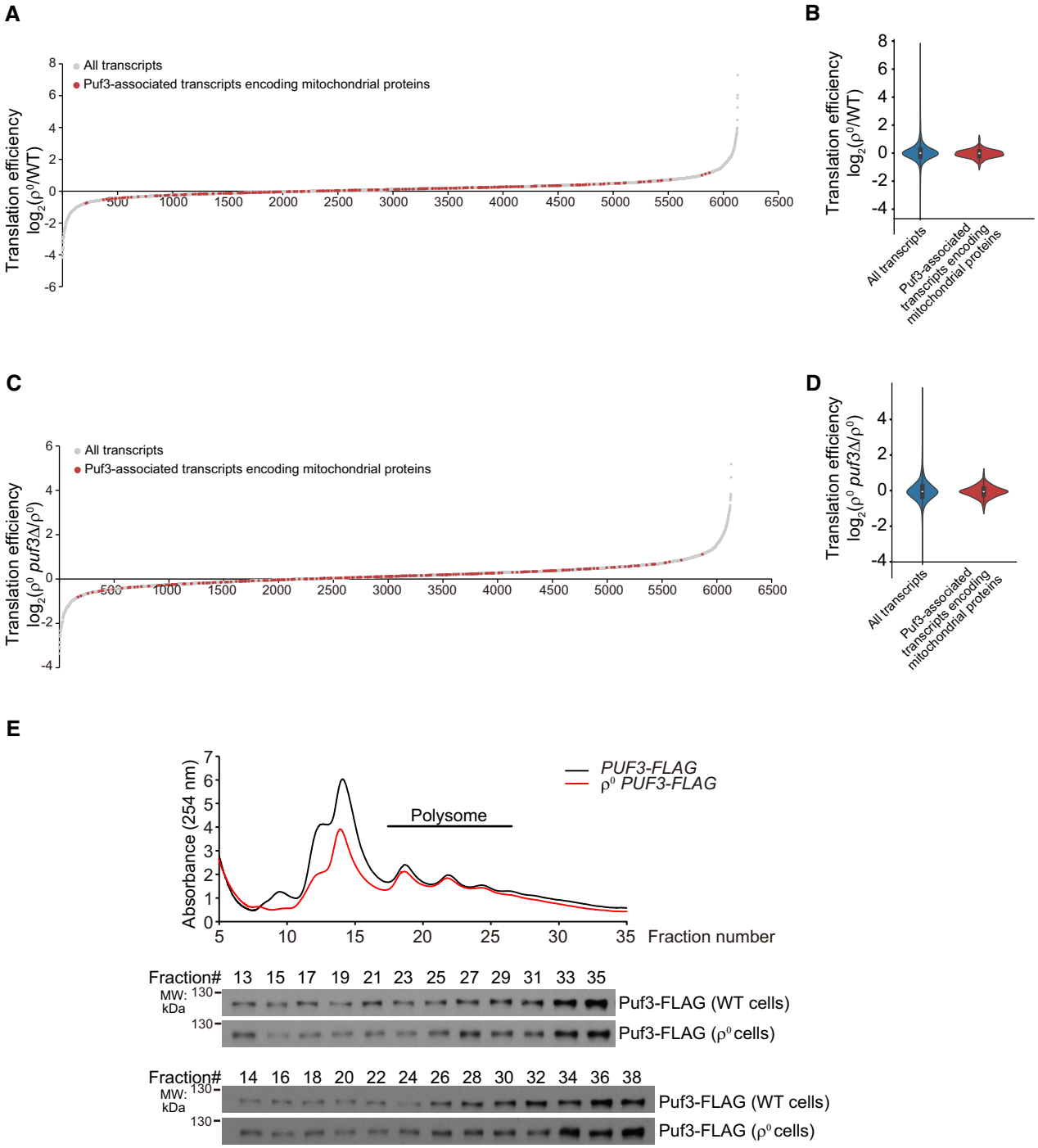

Figure EV4. Ribosome footprinting and polysome analysis. Related to Fig 4.

A Genome-wide translation efficiency changes of ρ^0 cells versus WT cells. The translation efficiencies of Puf3-associated mitochondrial transcripts are highlighted in red. Translation efficiency was determined by ribosome footprinting (Dataset EV3).

B Violin plot of translation efficiency changes of ρ^0 versus WT cells.

C Genome-wide translation efficiency changes of ρ^0 *puf3*Δ versus ρ^0 cells. Translation efficiency was determined by ribosome footprinting (Dataset EV3).

D Violin plot of translation efficiency changes of ρ^0 *puf3*Δ cells versus ρ^0 cells.

E Polysome analysis of Puf3-FLAG. Equal volume of lysates from the indicated fractions was loaded for Western blot analysis.

Source data are available online for this figure.

© 2021 The Authors

A

Peptide coverage of Puf3 (70%)

```
  1 MEMNMDMDMDMELASIVSSLSALSHSNNNGGQAAAAGIVNGGAAGSQQIG
 51 GFRRSSFTTANEVDSEILLLHGSSESSPIFKKTALSVGTAPPFSTNSKKF
101 FGNGGNYYQYRSTDTASLSSASYNNYHTHHTAANLGKNNKVNHLLGQYSA
151 SIAGPVYYNGNDNNNSGGEGFFEKFGKSLIDGTRELESQDRPDAVNTQSQ
201 FISKSVSNASLDTQNTFEQNVESDKNFNKLNRNTTNSGSLYHSSSNSGSS
251 ASLESENAHYPKRNIWNVANTPVFRPSNNPAAVGATNVALPNQQDGPANN
301 NFPPYMNGFPPNQFHQGPHYQNFPNYLIGSPSNFISQMISVQIPANEDTE
351 DSNGKKKKKANRPSSVSSPSSPPNNSPFPFAYPNPMMFMPPPPLSAPQQQ
401 QQQQQQQQQEDQQQQQQQENPYIYYPTPNPIPVKMPKDEKTFKKRNNKNH
451 PANNSNNANKQANPYLENSIPTKNTSKKNASSKSNESTANNHKSHSHSHP
501 HSQSLQQQQQTYHRSPLLEQLRNSSSDKNSNSNMSLKDIFGHSLEFCKDQ
551 HGSRFIQRELATSPASEKEVIFNEIRDDAIELSNDVFGNYVIQKFFEFGS
601 KIQKNTLVDQFKGNMKQLSLQMYACRVIQKALEYIDSNQRIELVLELSDS
651 VLQMIKDQNGNHVIQKAIETIPIEKLPFILSSLTGHIYHLSTHSYGCRVI
701 QRLLEFGSSEDQESILNELKDFIPYLIQDQYGNYVIQYVLQQDQFTNKEM
751 VDIKQEIIETVANNVVEYSKHKFASNVVEKSILYGSKNQKDLIISKILPR
801 DKNHALNLEDDSPMILMIKDQFANYVIQKLVNVSEGEGKKLIVIAIRAYL
851 DKLNKSNSLGNRHLASVEKLAALVENAEV*
```

S/T: phosphorylation sites quantified in B
S: phosphorylation sites not quantified in B due to low phosphorylation level or low peptide number

B

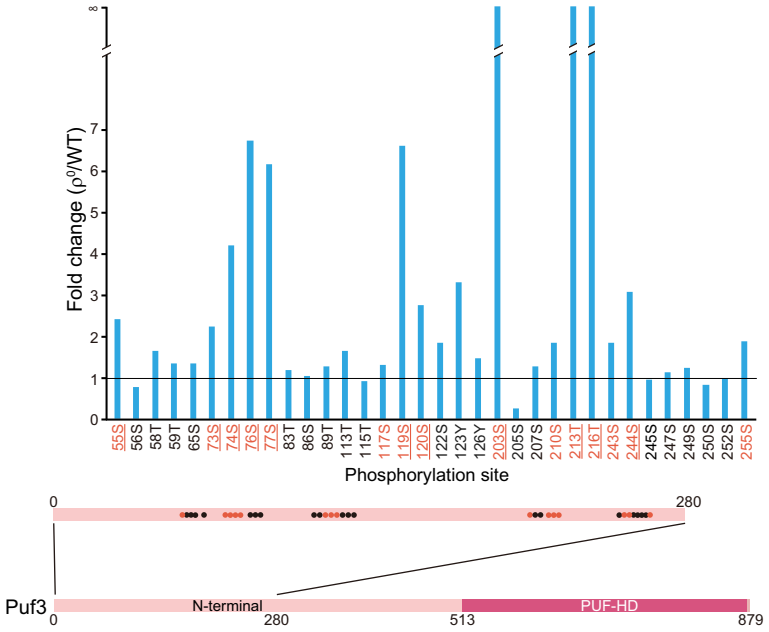

Figure EV5. SILAC analysis of Puf3 phosphorylation. Related to Fig 5.

A Peptide coverage map of Puf3. Peptide sequences covered by mass spectrometry are shown in red. Underlined residues are phosphorylated. Blue underlined residues: phosphorylation sites quantitatively analyzed in Fig EV5B. Green underlined residues: phosphorylation sites not quantitatively analyzed due to low phosphorylation level or low total peptide number. Mass spectrometry data are shown in Dataset EV6.

B Quantitative analysis of Puf3 site-specific phosphorylation (ρ^0 versus WT). The localization of phosphorylation sites at the N terminus of Puf3 is illustrated. Residues mutated in Puf3-15A are highlighted in red. Residues mutated in Puf3-11A are highlighted in red and underlined. The horizontal line indicates fold change of 1.

© 2021 The Authors